

1 **Inter-comparison of online and offline methods for measuring ambient heavy and trace elements**
2 **and water-soluble inorganic ions (NO₃⁻, SO₄²⁻, NH₄⁺ and Cl⁻) in PM_{2.5} over a heavily polluted**
3 **megacity, Delhi**

4 Himadri Sekhar Bhowmik¹, Ashutosh Kumar Shukla¹, Vipul Lalchandani¹, Jay Dave², Neeraj Rastogi²,
5 Mayank Kumar³, Vikram Singh⁴, and Sachchida Nand Tripathi^{1*}

6 ¹ Department of Civil Engineering, Indian Institute of Technology Kanpur, Kanpur, India

7 ^{1*} Department of Civil Engineering and Centre for Environmental Science and Engineering, Indian
8 Institute of Technology Kanpur, Kanpur, India

9 ² Geosciences Division, Physical Research Laboratory, Ahmedabad, India

10 ³Department of Mechanical Engineering, Indian Institute of Technology Delhi, New Delhi, India

11 ⁴Department of Chemical Engineering, Indian Institute of Technology Delhi, New Delhi, India

12 *Correspondence to:* S. N. Tripathi (snt@iitk.ac.in)

13 **Keywords:** Aerosol mass spectrometer (AMS), Xact 625i ambient metal mass monitor, Ion
14 Chromatography (IC), ICP-MS, elemental composition.

15 **Abstract**

16 Characterizing the chemical composition of ambient particulate matter (PM) provides valuable
17 information on the concentration of secondary species, toxic metals and assists in the validation of
18 abatement techniques. The chemical components of PM can be measured by sampling on filters and
19 analysing them in the laboratory or using real-time measurements of the species. It is important for the
20 accuracy of the PM monitoring networks that measurements from the offline and online methods are
21 comparable and biases are known. The concentrations of water-soluble inorganic ions (NO₃⁻, SO₄²⁻, NH₄⁺
22 and Cl⁻) in PM_{2.5} measured from the 24 hrs filter samples using ion chromatography (IC) were compared
23 with the online measurements of inorganics from aerosol mass spectrometer (AMS) with a frequency of 2
24 mins. Also, the concentrations of heavy and trace elements determined from the 24 hrs filter samples
25 using inductively coupled plasma mass spectroscopy (ICP-MS) were compared with the online
26 measurements of half-hourly heavy and trace metal's concentrations from Xact 625i ambient metal mass
27 monitor. The comparison was performed over two seasons (summer and winter) and at two sites (Indian
28 Institute of Technology, Delhi and Indian Institute of Tropical Meteorology, Delhi) which are located in

29 Delhi, NCR, India, one of the heavily polluted urban areas in the world. Collocated deployments of the
30 instruments helped to quantify the differences between online and offline measurements and evaluate the
31 possible reasons for positive and negative biases. The slopes for SO_4^{2-} and NH_4^+ were closer to 1:1 line
32 during winter and decreased during summer at both sites. The higher concentrations on the filters were
33 due to the formation of particulate $(\text{NH}_4)_2\text{SO}_4$. Filter-based NO_3^- measurements were lower than online
34 NO_3^- during summer at IITD and winter at IITMD due to the volatile nature of NO_3^- from the filter
35 substrate. Offline measured Cl^- was consistently higher than AMS derived Cl^- during summer and winter
36 at both sites. Based on their comparability characteristics, elements were grouped under 3 categories. The
37 online element data were highly correlated ($R^2 > 0.8$) with the offline measurements for Al, K, Ca, Ti, Zn,
38 Mn, Fe, Ba, and Pb during summer at IITD and winter at both the sites. The higher correlation
39 coefficient demonstrated the precision of the measurements of these elements by both Xact 625i
40 and ICP-MS. Some of these elements showed higher Xact 625i elemental concentrations than ICP-MS
41 measurements by an average of 10-40% depending on the season and site. The reasons for the differences
42 in the concentration of the elements could be the distance between two inlets for the two methods, line
43 interference between two elements in Xact measurements, sampling strategy, variable concentrations of
44 elements in blank filters and digestion protocol for ICP measurements.

45 **1. Introduction**

46 The adverse effect of ambient particulate matter (PM) on human health and the role of PM in visibility
47 degradation, altering earth's radiation balance, and climate change has received global attention in the last
48 two decades (Pope et al., 2009; Hong et al., 2019; Wang et al., 2019). To gain better insight into their
49 properties, the chemical characterization of particulate matter and its source attribution is crucial. The
50 National Capital Region (NCR), which includes India's capital (New Delhi) along with some districts
51 (Gurugram, Faridabad, and Noida) of the adjoining states of Haryana, Rajasthan, and Uttar Pradesh, is one
52 of the most polluted urban areas in northern India with a population over 47 million (Bhowmik et al.,
53 2021). According to World Economic Forum, New Delhi was listed as the most polluted city globally,
54 with an annual average $\text{PM}_{2.5}$ concentration of $\sim 140 \mu\text{g m}^{-3}$ (World Health Organisation, 2018). NCR has
55 been a specific area for researchers for the past couple of years due to its unprecedented $\text{PM}_{2.5}$ levels.
56 Various large and small scale industries, power plants, construction activities, and rapid increase in the
57 vehicle numbers (11 million in 2018) (Rai et al., 2020) are among the several causes that massively
58 reduces the air quality index (AQI) (Rai et al., 2020; Sharma & Kulshrestha, 2014). Further, the crop
59 residue burning during the month of Oct-Nov in the adjoining states of Haryana and Punjab on a larger
60 scale worsens the air quality.

61 For decades, the mass concentrations of major water soluble inorganic ions (WSIS) and heavy and trace
62 metals in PM have been carried out by sampling them on filters and subsequently analysing them in
63 laboratory. Water-soluble inorganic ions (WSIS) and heavy and trace elements from these filter samples
64 are analyzed using ion chromatography (IC) (Bhowmik et al., 2021; Rengarajan et al., 2007; Rastogi &
65 Sarin, 2005) and inductively coupled plasma-mass spectroscopy (ICP-MS) or inductively coupled
66 plasma-optical emission spectroscopy (ICP-OES) (Patel et al., 2021) respectively. Usually, these filters
67 are collected over 24 hrs interval. Traditional receptor models usually use these offline measured data of
68 very low temporal resolution, making it challenging to characterize the short pollution episodes and
69 dynamics of pollution sources. Further, un-denuded filter sampling can have both negative and positive
70 artifacts due to volatile species (Lipfert, 1994; Pathak & Chan, 2005). The absorption of acidic and
71 alkaline gases on the filter substrates, if not removed prior to sampling, can give positive artifacts and
72 result in overestimating species concentration. Likewise, the evaporation of semi-volatile compounds
73 (ammonium nitrate) from filter substrates can give negative biases and result in underestimating aerosol
74 concentration and its species (Pathak and Chan, 2005; Zhang and McMurry, 1992). The degree of
75 artifacts can be affected by several factors, including temperature, relative humidity, type of filter
76 substrate, the aerosol loading on the filter substrate, etc. Transient events can also lead to mismatch. To
77 overcome the limitations of low temporal resolution and avoid the artifacts associated with offline filter
78 sampling, methods have been developed for measuring aerosol chemical composition at a higher time
79 resolution in the order of hours or minutes.

80 Aerosol Mass Spectrometer (AMS) (Canagratna et al., 2007; Jayne et al., 2000; Jimenez et al., 2003) is
81 one kind of such instrument, which provides size-resolved chemical composition of non-refractory
82 submicron aerosols, e.g., organics, sulphate, nitrate, ammonium, and chloride at the order of hours or
83 even minutes. For other important components, such as calcium (main constituents of soil dust and
84 construction activities) and potassium (tracer of biomass burning), which AMS cannot measure, Xact
85 ambient metal mass monitor can be used. It is capable of measuring 45 elements, e.g., Al, Si, P, S, Cl, K,
86 Ca, Ti, V, Cr, Mn, Fe, Co, Ni, Cu, Zn, Ga, Ge, As, Se, Br, Rb, Sr, Y, Zr, Nb, Mo, Pd, Ag, Cd, In, Sn, Sb,
87 Te, I, Cs, Ba, La, Ce, Pt, Au, Hg, Tl, Pb and Bi with a frequency of every 30 mins to 4 hours. However,
88 the high time-resolution instruments measure lower range of species concentrations with higher limit of
89 detection (LOD) than the offline based methods (Tremper et al., 2018). Both offline and online methods
90 have their own strength and weaknesses. Uncertainties in offline filter analysis methods have been
91 extensively studied (Pathak and Chan, 2005; Viana et al., 2006), but the novel online methods pose new
92 problems (Wu and Wang, 2007). For example, when the ambient concentrations are very low, online
93 measurements are often close to the MDL values due to the short integration times (Malaguti et al., 2015).

94 Previous studies in Delhi-NCR have used low time resolution filter-based methods for chemical
95 characterization of submicron aerosols (Bhowmik et al., 2020; Nagar et al., 2017; Pant et al., 2015;
96 Sharma et al., 2016; Singhai et al., 2017). On the other hand, there are only a few studies in Delhi-NCR
97 that used high time resolution methods (HR-ToF-AMS, Q-ACSM, Xact) for characterization and source
98 apportionment of coarse and fine particulate matters (Gani et al., 2019; Lalchandani et al., 2021; Rai et
99 al., 2020, 2021; Singh et al., 2021; Tobler et al., 2020). Online and offline measurements both have their
100 advantages and limitations. For both these measurements, the quality of the data highly depends on the
101 calibration of the instruments. For Xact, the multi-element mix standard might not represent ambient
102 elemental mix if the ambient particulate matters are too low or too high in concentration, affecting the
103 collection properties of the filter (Indresand et al., 2013). For filter-based water-soluble inorganic ion and
104 metal analysis, confidence in the data depends on the calibration as well as the volatility, solubility, and
105 digestion protocol used for the extraction of water-soluble inorganic ions and elements, respectively.
106 Thus, it is vital for monitoring networks that both the offline and online measurement methods give
107 comparable results. Few published studies have compared inorganics and elements from filter-based
108 measurements and semi-continuous methods (e.g., Furger et al., 2017; Nie et al., 2010). The inter-
109 comparison in these studies is unjustified for highly polluted areas, as the specie values observed in these
110 studies are much below MDL due to very low ambient concentration of secondary species and elements.
111 It will be interesting to study the inter-comparison in highly polluted areas. To the best of our knowledge,
112 there are neither any published seasonal and temporal comparisons of inorganics from high time
113 resolution AMS measurements and filter-based measurements from ion chromatography nor any
114 comparisons of heavy and trace metals from high time resolution Xact 625 ambient metal mass monitor
115 and offline measurements from ICP-MS in the heavily polluted Delhi NCR region.

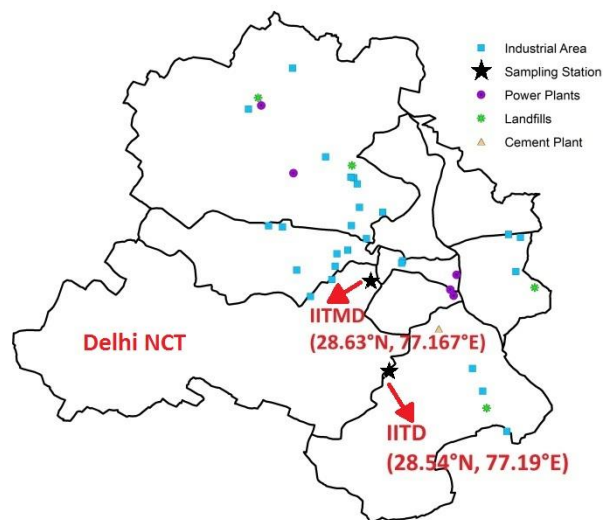
116 This study demonstrates a comparison between online and offline measurements of WSIS and heavy and
117 trace metals at two sites in Delhi NCR during summer (June-July 2019), characterized by moderate levels
118 of local pollution and winter (October-December 2019), affected by high levels of pollution from local
119 sources and regional transport of crop residue burning emissions from adjoining state of Haryana and
120 Punjab.

121 **2. Methodology**

122 **2.1. Sampling sites**

123 Delhi-NCR, a highly polluted urban area with an annual average $PM_{2.5}$ concentration of $140 \mu g m^{-3}$ and a
124 population of over 47 million, is surrounded by the Thar desert on its west and Indo-Gangetic Plain on its

125 east to south-east. The temperature is about $\sim 35^{\circ}\text{C}$ - 48°C during summer (April-June), and winter
126 (December-February) is relatively cooler, with temperature ranges from $\sim 2^{\circ}\text{C}$ - 15°C (Bhowmik et al.,
127 2020; Lalchandani et al., 2021; Tobler et al., 2020). The wind is mostly north-westerly during both
128 summer and winter.



129

130 Fig.1. Sampling sites with various emission sources like power plants, industries, landfills, etc.

131 2.1.1. Delhi NCR site 1: IITD

132 High volume $\text{PM}_{2.5}$ samples were collected on the rooftop of the Centre for Atmospheric Science (CAS)
133 building at the Indian Institute of Technology, Delhi (IITD) (28.54°N , 77.19°E ; ~ 218 m amsl) about ~ 15
134 m above the ground level. Further, one HR-ToF-AMS and Xact ambient metal mass monitor were
135 deployed inside a temperature-controlled laboratory on the 3rd floor of the same building about ~ 10 m
136 above the ground level. It is an educational institute as well as residential campus having restaurants
137 nearby and very close to (< 200 m) heavy traffic road. Lalchandani et al., (2021); Rai et al., (2020)
138 observed source signatures of emissions from industries, power plants, vehicles, and waste burning in this
139 site.

140 2.1.2. Delhi NCR site 2: IITMD.

141 Offline $\text{PM}_{2.5}$ sampling was carried out on the rooftop of the main building at the Indian Institute of
142 Tropical Meteorology Delhi (IITMD) (28.63°N , 77.167°E ; ~ 220 m above msl) about 15 m above the
143 ground level. Moreover, HR-ToF-AMS and Xact ambient metal mass monitor were installed inside a

144 temperature-controlled laboratory on the 2nd floor of the same building at the height of ~8 m from the
145 ground level. This site is placed in the central urban area of Delhi and surrounded by Central Ridge
146 reserve forest and residential areas (Tobler et al., 2020) and around 14 km away in North West direction
147 from IITD. A recent study by Lalchandani et al. (2021) observed the site is dominated by emissions from
148 traffic, solid fuel burning, and oxidized organic aerosols. The location of the sampling sites are shown in
149 Fig. 1.

150 **2.2. Sampling details**

151 **2.2.1 Offline sampling**

152 Biweekly 24 hrs (January-May and August-September 2019) and daily 24 h (June-July and October-
153 December 2019) PM_{2.5} samples were collected on quartz filter substrates (Whatman; 8 × 12 inches) using
154 a high-volume sampler (HVS) with a flow rate of 1.13 m³/min. Blanks were collected in the field by
155 placing a fresh filter in the sampler while not running. A total of 64 filters (60 from IITD site during June-
156 July 2019 including 4 blanks) were collected in summer whereas, a total of 186 filters (90 from each site
157 during October-December 2019 plus 6 blanks) were collected in winter. The collected filters, including
158 field blanks, were zip-locked and stored in the freezer at each site and periodically transported to CESE
159 (Centre for Environmental Science and Engineering), IIT Kanpur, where they were further stored at -20°C
160 in a deep freezer prior to analysis. For this study, the samples from the common period of offline and
161 online sampling (October-December 2019) from the two sites were analyzed for WSIS (SO₄²⁻, NO₃⁻, NH₄⁺
162 and Cl⁻) using an IC, and 32 metals (Al, Na, K, Ca, Ti, V, Cr, Mn, Fe, Ni, Cu, Zn, As, Se, Rb, Sr, Zr, Cd,
163 Sn, Sb, Ba, Pb, Cs, La, Ce, Pt, Tl, Mg, Li, Mo, Co and Pd) using an ICP-MS. More details of analytical
164 procedures are given in the instrumentation section.

165 **2.2.2 Online sampling**

166 At both IITD and IITMD site, high-resolution time-of-flight aerosol mass spectrometers (HR-ToF-AMS,
167 Aerodyne Research Inc., Billerica, MA) (Canagaratna et al., 2007; DeCarlo et al., 2006), equipped with
168 PM_{2.5} aerodynamic lens (Peck et al., 2016) (Aerodyne Research Inc., Billerica, MA, USA) were installed
169 inside air-conditioned laboratories. Ambient fine particulate matters were sampled through PM_{2.5} cyclone
170 (BGI, Mesa Labs. Inc.) inlet at IITD with a flow rate of 5 lpm (l/min) using a 2.44 m long stainless-steel
171 tubing (0.3 inch I.D and 0.4 inch O.D) and through black silicon tubing (0.19 inch I.D) at IITMD, placed
172 1.5 m above the rooftop. A Nafion dryer (MD-110-144P-4; Perma Pure, Halma, UK) was used to dry the
173 ambient aerosols to maintain the output RH at 20%. At IITD, data were collected from 12th October 2019-

174 31st December 2019 and 2nd June 2019-21st July 2019 during winter and summer campaigns respectively.
 175 The data between 1st November and 14th November was not available, due to hardware issues in the AMS
 176 during that period. At IITMD, data were only collected during winter campaign from 25th October 2019 to
 177 31st December 2019.

178 Two Xact 625i ambient metal monitors (Cooper Environmental Services, Beaverton, Oregon, USA) were
 179 installed inside temperature controlled laboratories at IITD and IITMD. Ambient aerosols were sampled
 180 through a PM_{2.5} inlet with a flow rate of 16.7 lpm. A separate sampling line of 2.44 meter (1.25 inch I.D)
 181 for the Xact which was made of aluminium was installed. A heater was set up at the end of the sampling
 182 line to ensure 45% RH set point. At IITD, sampling was carried out from 1st October 2019-31st December
 183 2019 and 30th May 2019-25th July 2019 during the winter and summer campaign, respectively. However,
 184 data between 16th July and 24th July were not available due to hardware breakdown. At IITMD, samples
 185 were collected from 1st October 2019-31st December 2019 but data from 18th November to 26th
 186 November 2019 and 30th November to 14th December 2019 were not available due to instrumental
 187 problems.

188 Online measurements of inorganic ions (SO₄²⁻, NO₃⁻, NH₄⁺ and Cl⁻) from HR-ToF-AMS were compared
 189 with the WSIS using an IC. Parallely, heavy and trace metals obtained from Xact ambient metal mass
 190 monitor were compared with the metal data from the offline filter measurements using an ICP-MS.
 191 Though the sampling periods of AMS, Xact, and HVS were different for different seasons and different
 192 sites as well (Table 1), only the common periods of online and offline sampling have been discussed in
 193 this study for comparison.

194 Table 1. Sampling strategy and instrumentation used.

	Interval	IITD	IITMD
Quartz filter Sampling	3 days	January-May 2019	January-May 2019
		August-September 2019	August-September 2019
	24 hrs	June-July 2019	June-July 2019
		October-December 2019	October-December 2019
HR-Tof-AMS	2 mins	2 nd June-21 st July 2019 12 nd October-31 st December 2019	25 th October-31 st December 2019
Xact	30 mins	30 th May-25 th July 2019 1 st October-31 st December 2019	1 st October-31 st December 2019

195 Filters from the common periods were analysed for WSIS and heavy and trace metals using an IC and ICP-MS respectively.

196 2.3. Instrument details

197 2.3.1 WSIS measurements by IC and HR-ToF-AMS

198 For WSIS analysis, 9 sq.cm punch area of each collected filter was soaked in 30 ml of high purity milli-q
199 water (resistivity-18.20 M Ω cm) for 12 hours in pre-cleaned borosilicate test tubes to ensure maximum
200 solubility. The amount of water added, soaking time, etc. effect the solubility of the ions as well as the
201 extent of extraction. Details can be found in our previous paper (Bhowmik et al., 2020). Soaked samples
202 were filtered through 0.22 μ m quartz filter papers to remove any suspended contaminations after an
203 ultrasonication for 50 mins. Cl⁻, NO₃⁻, SO₄²⁻ and, NH₄⁺ were measured for all the filter extracts by an IC
204 (Metrohm 883 Basic IC plus for cations and 882 compact IC plus for anions). Separate columns for the
205 analysis of cations and anions were installed in two separate modules. For anion and cation separation, an
206 AS 5-250/4.0 chromatography column and C-6 column was used, respectively. The sample carried by 3.2
207 mM Na₂CO₃+1 mM NaHCO₃ solution and 2.7 mM HNO₃ solution in the anion and cation module
208 separately passes through the charged columns to analyze each ion according to their polarity. The
209 calibration was performed by a seven-point method with a range of standards prepared by the serial
210 dilution from the stock solution standard of 10 ppm purchased from Metrohm. The uncertainty of the
211 water-soluble inorganic ions measured by IC was estimated as 4% (coverage factor~2) by the approach
212 described in Yardley et al. (2007).

213 HR-ToF-AMS measures size-resolved mass spectra of non-refractory particles (PM components that
214 vaporize at 600°C and 10⁻⁵ Torr, e.g., organics, nitrate, sulphate, ammonium, and some chlorides) of
215 submicron particulate matters. The details of this instrument can be found elsewhere (DeCarlo et al.,
216 2006). Briefly, ambient aerosols are collected through an orifice of 100 μ m diameter and focused into a
217 narrow particle beam by an aerodynamic lens system installed inside the instrument, which has a
218 transmission efficiency of > 50% for PM_{2.5} (DeCarlo et al., 2006; Peck et al., 2016). The particle size is
219 determined after analyzing the time of flight, i.e., time taken to travel along the length of the sizing
220 chamber. The NR-PMs are then vaporized by hitting the vaporizer at 600°C and at a vacuum of 10⁻⁷ Torr.
221 Further, the vaporized molecules are electronically ionized at 70 eV, followed by detection by a mass
222 spectrometer as per their *m/z*. HR-ToF-AMS can be operated in W-mode or V-mode. For this study, it
223 was operated in V-mode with a sampling time of 2 mins. Mass spectra (MS) mode, in which mass spectra
224 of the components are measured, and particle time-of-flight (PToF) mode in which the size-resolved mass
225 spectra are measured, are alternated in every 30s in 2 cycles. The HR-ToF-AMS was calibrated using
226 standard protocols provided in our previous publication (Lalchandani et al., 2021; Singh et al., 2019).

227 To determine the mass concentration of NR-PMs, Unit mass resolution (UMR) analysis was done using
228 the SQUIRREL data analysis toolkit (version 1.59) programmed in IGOR Pro 6.37 software
229 (Wavemetrics, Inc., Portland, OR, USA). High resolution (HR) analysis was also done on the data set
230 using Peak Integrated Key Analysis (PIKA version 1.19) toolkit. A recommended collection efficiency
231 (CE) of 1 (Hu et al., 2017) was used for capture vaporizer. At the beginning and mid of each campaign at
232 the two sites, ionization efficiency (IE) calibration was performed by injecting mono-disperse 300 nm
233 ammonium nitrate and ammonium sulphate particles into AMS and a condensation particle counter
234 (Jayne et al., 2000). A relative ionization efficiency (RIE) of 4.05 and 4.35 was used for IITD and IITMD
235 site, respectively in case of NH₄. RIE of SO₄ was taken as 2.89 and 1.67 for IITD and IITMD,
236 respectively. For Org and Cl, by default a RIE of 1.4 and 1.3 were taken, respectively. More details can
237 be found in (Lalchandani et al., 2022).

238 **2.3.2 Heavy and trace metal measurements by ICP-MS and Xact 625i**

239 For the analysis of heavy and trace metals, 15 sq. cm area of each collected filter was digested in an acid
240 mix of 0.5 ml HF+1.5 ml HNO₃ for 4 hours within closed HDPE Teflon tubes using a Hot plate (Savillex-
241 HF resistive Model number 88888:00000). The temperature range should be ~90-120°C to ensure
242 complete digestion of the elements. Further, 2.5 ml of HClO₄ was added to the precipitates, left over the
243 Teflon tube wall and the tubes were kept on the hot plate at 220-240°C for another 4 hours with the lids
244 open for complete evaporation of the acid mix. Moreover, the residual was dissolved in 6N HNO₃ and
245 diluted with de-ionized water (resistivity-18.20 MΩ cm) followed by filtering through 0.22 μm quartz
246 filter papers prior analysis. Details can be found in our forthcoming paper. This method is well
247 established and used in many studies (Minguillón et al., 2012; Querol et al., 2008).

248 Thirty two metals (Al, Na, K, Ca, Ti, V, Cr, Mn, Fe, Ni, Cu, Zn, As, Se, Rb, Sr, Zr, Cd, Sn, Sb, Ba, Pb,
249 Cs, La, Ce, Pt, Tl, Mg, Li, Mo, Co and Pd) were analyzed for all filter extracts using an ICP-MS (Thermo
250 Scientific iCAP Q ICP-MS) at IIT Kanpur Environmental Engineering laboratory. Si could not be
251 determined in the filter samples because Si is the primary constituent of the quartz filters and hence
252 digested during sample preparation. Samples were first introduced to a nebulizer using an injector
253 attached to an autosampler for transformation into fine aerosol droplets followed by ionization at a very
254 high temperature (8000K) in Ar-plasma. The elements elute as per their *m/z*. A known concentration (5
255 ppb) of Ge was used as an internal standard to monitor the instrumental drift during the analysis. The
256 overall average drift was reported as ± 10%. The calibration was performed by ten-point method with a
257 range of mix standards prepared by the serial dilution from the High purity multi-element (35 elements)
258 standards (soluble in 1% HNO₃, 100 ppm) purchased from Sigma Aldrich.

259 The Xact 625i Ambient Metals Monitor (Cooper Environmental Services (CES), Beaverton, OR, USA)
260 uses X-ray fluorescence to measure the real-time elemental data in particulate matter. For this study, a
261 PM_{2.5} inlet was used. Details of the instrument can be found in Furger et al., 2017. Briefly, aerosol
262 samples were collected on a Teflon filter tape followed by hitting the loaded area with X-rays and the
263 fluorescence measured by a silicon drift detector (SDD). Thirty elements: Al, Si, S, Cl, K, Ca, Ti, Cr, Mn,
264 Fe, Co, Ni, Cu, Zn, As, Se, Br, Rb, Sr, Zr, Mo, Cd, In, Sn, Sb, Te, Ba, Pb, Bi, and Bi were measured with
265 30 min time resolution. The Xact 625i was calibrated during each campaign using thin film standards for
266 the individual elements. The reproducibility was observed within $\pm 5\%$. Every midnight energy alignment
267 checks were performed for 15 mins (00:15 to 00:30) (for Cr, Pb, Cd and Nb). An uncertainty of $\sim 10\%$
268 was reported by the manufacturer in an interference free situation (USEPA & Etv, 2012). This included
269 1.73% from flow (CEN, 2014), 5% for standard reproducibility or uncertainty during calibration
270 (USEPA, 1999) and 2.9% from term stability as reported in Tremper et al. (2018). More details on the
271 instrumental set up and stability check during the summer and winter campaign can be found in Rai et al.
272 (2020) and Shukla et al. (2021).

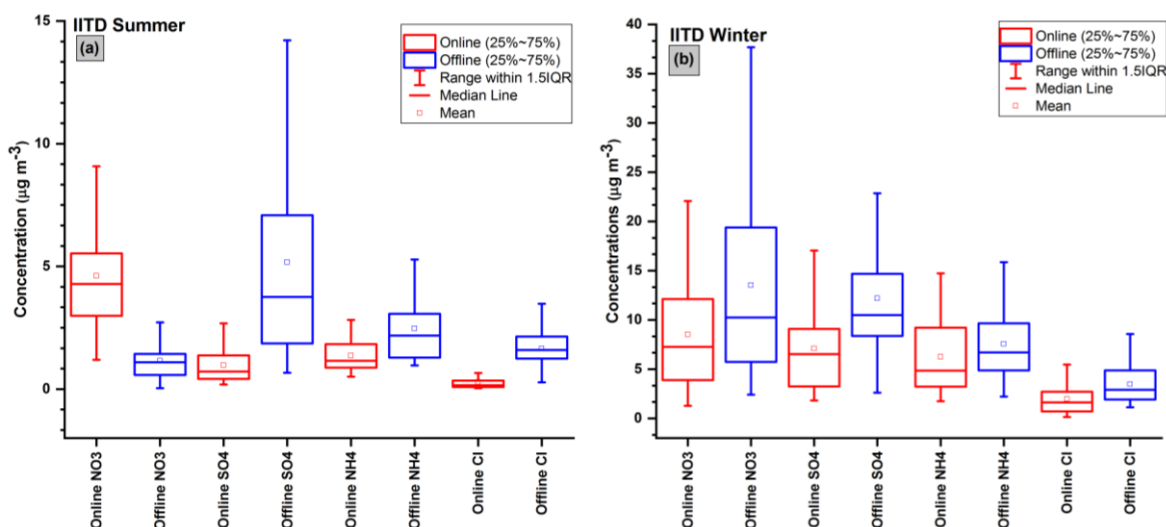
273 **3. Results and discussions**

274 **3.1. Online and offline measurements of WSIS and their comparison**

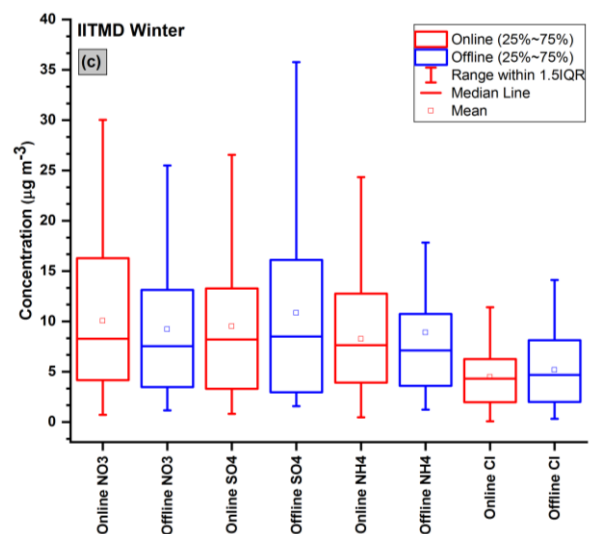
275 Large temporal variability was observed in both offline and online measurements of WSIS (NO_3^- , SO_4^{2-}
276 and, NH_4^+ and Cl^-) during the winter campaign and summer campaign at both sites. The inorganics data
277 with 2 mins interval from HR-ToF-AMS were averaged over the sampling period of the filters, i.e., 24
278 hours. The time series of NO_3^- , SO_4^{2-} , NH_4^+ , and Cl^- during the summer and winter campaign at IITD and
279 winter campaign at IITMD are shown in Fig. SM1 in the supplementary material. Higher peaks of
280 inorganics were observed during 25th Oct-18th Nov during the winter campaign at IITD, which was the
281 agricultural crop-residue burning period (Nagar et al., 2017). During the winter campaign, NO_3^- was the
282 most abundant ion followed by SO_4^{2-} , NH_4^+ and Cl^- for both offline and online measurements at both the
283 sites whereas, during the summer campaign at IITD, NO_3^- was the most abundant ion followed by NH_4^+ ,
284 SO_4^{2-} and Cl^- in online measurement (HR-ToF-AMS). Similar results were observed in our companion
285 paper, Shukla et al. (2021). Interestingly, in the case of offline measurements during the summer
286 campaign at IITD, NO_3^- was least abundant, and the sequence changed as $\text{SO}_4^{2-} > \text{NH}_4^+ > \text{Cl}^- > \text{NO}_3^-$. The
287 average concentrations with their ranges are tabulated in Table SM1 in supplementary material, and the
288 mean, maximum and minimum concentration are shown in Fig. 2 using box plots.

289 Comparability and correlation between offline and online measurements were evaluated in this study by
 290 applying linear regression using offline data as the independent and online data as the dependent variable.
 291 The comparability of NH_4^+ measurements was observed to be good for both summer and winter
 292 campaigns at both sites. During the winter campaign, the correlations were $R^2=0.76$, and $R^2=0.89$, and the
 293 slopes were closer to 1 (0.99 for IITD and 0.93 for IITMD) for IITD and IITMD, respectively (Fig. 3).
 294 Interestingly during the summer campaign at IITD, though the correlation improves ($R^2=0.91$), the slope
 295 decreases to 0.49. This is likely because the vapor concentration of sulfuric acid (H_2SO_4) is higher during
 296 summers. As a result of which, the adsorption of sulfuric acid on PM deposited on the filter papers
 297 happens during summers which reacts with gaseous ammonia (NH_3) to form a relatively stable particulate
 298 $(\text{NH}_4)_2\text{SO}_4$ (Zhang et al., 2000), thus increasing ammonium concentration in the offline measurements
 299 during the warmer season, especially in the presence of dust (Nicolás et al., 2009).

300

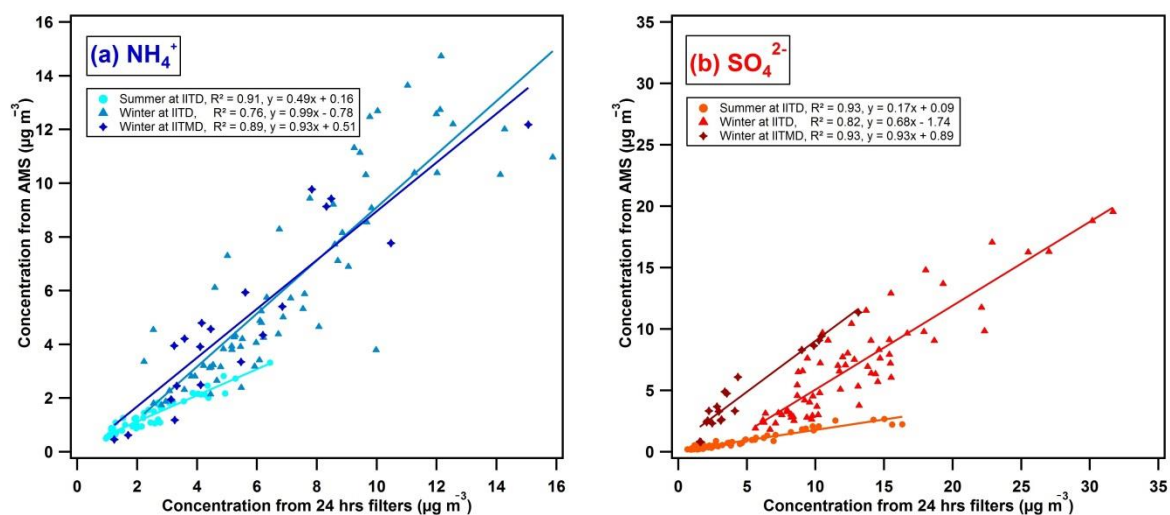


301

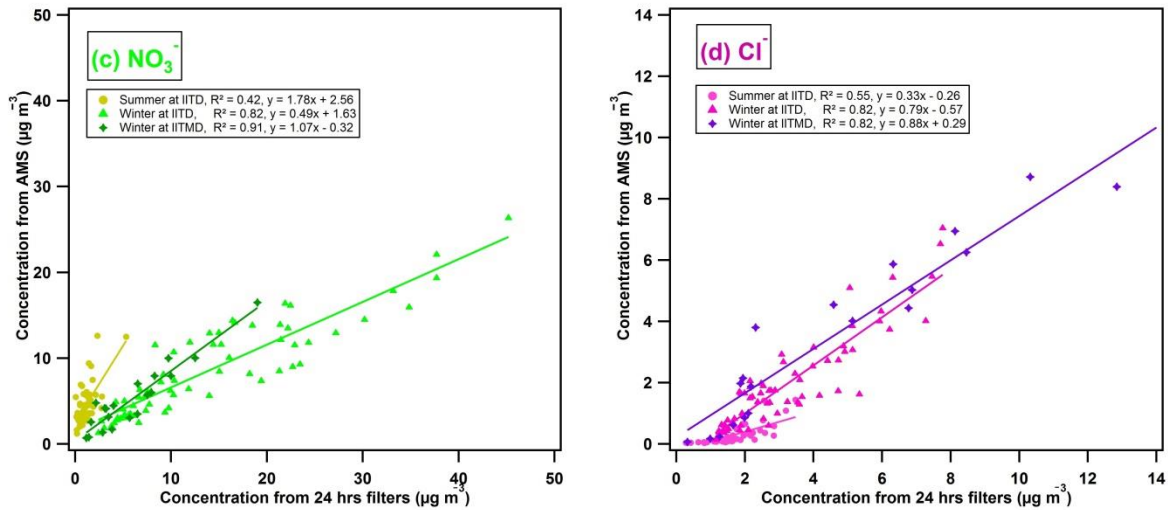


302 Fig.2. Box plots of online and offline measured secondary species (NO_3^- , SO_4^{2-} and, NH_4^+) and Cl^- during
 303 (a) summer campaign at IITD, (b) winter campaign at IITD, and (c) winter campaign at IITMD site.

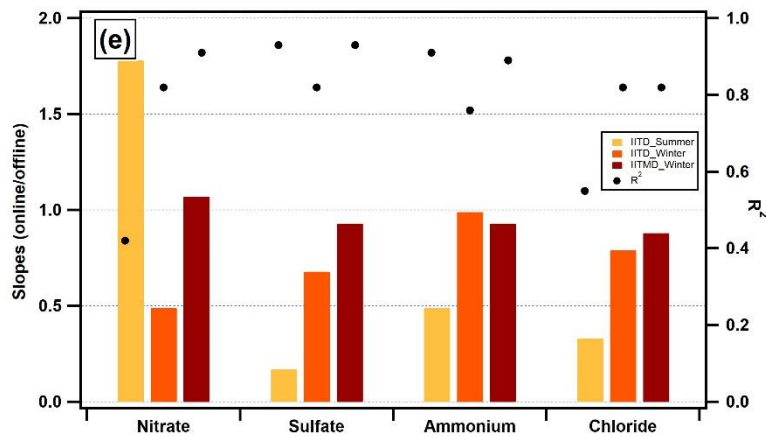
304 The filter-based measurements of SO_4^{2-} were higher than those from the online measurements for IITD
 305 and IITMD during both the seasons (Fig. 2). Their comparability is characterized by a correlation
 306 coefficient of $R^2=0.93$ with a slope of 0.17 and $R^2=0.82$ with a slope of 0.68 at IITD during the summer
 307 and winter campaigns, respectively. Interestingly, offline SO_4^{2-} data correlates well with online SO_4^{2-} data
 308 having a correlation coefficient of $R^2=0.93$ with a slope close to 1 (0.93) during the winter campaign at
 309 IITMD (Fig. 3). A slope of less than 0.5 was observed in Malaguti et al., (2015) in Italy during the warm
 310 period whereas the offline measurement of SO_4^{2-} was 34% lesser than the AMS measurements in Pandolfi
 311 et al., (2014). The higher SO_4^{2-} concentrations on the un-denuded offline filter-based measurements could
 312 be due to refractory sulfate (e.g., potassium or calcium sulfate). The higher filter-sulfate could also be
 313 possibly because of the positive sampling artifact. The SO_2 is absorbed on the filter by the collected
 314 alkaline particles (Nie et al., 2010). The higher concentration could also be due to the formation of
 315 ammonium bi-sulfate or ammonium sulfate because of the reaction between gas-phase ammonia with the
 316 acidic aerosols (Nicolás et al., 2009). Also, the un-denuded filter measurements could lead to higher
 317 filter-sulfate. The interaction of gas phase ammonia with acidic aerosols can be minimized by using
 318 denuders while collecting aerosols on the filters (Nault et al., 2020). Some studies suggested that the
 319 organic sulfate, nitrate, and reduced nitrogen thermally decompose and/or under electron ionization in
 320 AMS, producing inorganic ions. NO^+ and NO_2^+ contribute a significant fraction in organic nitrate (Day et
 321 al., 2022) whereas, for organic sulfates, a large fraction of the signal is contributed by SO^+ , SO_2^+ , and
 322 SO_3^+ (Chen et al., 2019). Though the additional inorganics are minimum, this could lead to possible
 323 marginal biases between the online and offline measurement of the inorganics.



324



325



326

327 Fig.3. Scatter plots between online and offline measured (a) NH_4^+ , (b) SO_4^{2-} , (c) NO_3^- , (d) Cl^-
 328 concentrations and (e) comparison of slopes (online/offline) and R^2 of the measured inorganic ions in
 329 $\text{PM}_{2.5}$ during summer and winter campaign at IITD and during winter campaign at IIITMD.

330 The online and offline NO_3^- measurements posed a good correlation during winter ($R^2 = 0.91$ and slope of
 331 1.07 at IITMD, $R^2 = 0.82$ and slope of 0.49 at IITD) whereas the correlation worsens during summer at
 332 IITD ($R^2 = 0.42$ and slope of 1.78) (Fig. 3). The slopes and correlation coefficient for the WSIS are listed
 333 in Table 2. The NO_3^- concentrations measured by the HR-ToF-AMS were higher than the offline data
 334 during summer at IITD and during winter at IITMD whereas, filter-based measurements of NO_3^- were
 335 higher during winter at IITD (Fig. 2). The higher offline NO_3^- concentrations during winter at IITD can be
 336 possibly because of the positive artifact due to the absorption of gas-phase nitric acid (HNO_3) on the filter
 337 (Chow, 1995). Many studies (Chow et al., 2008; Kuokka et al., 2007; Malaguti et al., 2015) reported
 338 higher concentrations of NO_3^- from high time resolution measurements than filter-based measurements

339 due to the evaporation of ammonium nitrate collected on filters over the duration of sample collection
 340 (Pakkanen & Hillamo, 2002; Schaap et al., 2004; Kuokka et al., 2007). Pandolfi et al. (2014) observed
 341 NO_3^- HR-AMS/Filter ratios of ~ 1.7 at Barcelona and Montseny in Europe. This evaporation loss
 342 increases with the decrease of humidity and the increase of temperature (Chow et al., 2008; Takahama et
 343 al., 2004). Also, complete evaporation may occur beyond 25°C (Schaap et al., 2004). Chow et al. (2008)
 344 observed the evaporation loss from quartz filter to be more than 80% during the warm season in central
 345 California. The high temperature (35°C - 48°C) during the long sampling hours (24 hours) may be a
 346 possible reason for the poor correlation between online and offline NO_3^- measurements during the
 347 summer campaign at IITD. Schaap et al. (2004) reported that the NO_3^- volatilization during a 24-h
 348 sampling period not only depends on the sampling instruments and ambient conditions, but also on
 349 sampling strategy. If the sampling strategy is evening-to-evening (24 hours), the samples will lose the
 350 night NO_3^- sampled during the night with the increasing temperature during the day. However, during
 351 morning-to-morning sampling strategy, the filters will collect the night NO_3^- quantitatively throughout the
 352 night, but the higher temperature in the afternoon of the previous day may promote the loss of afternoon
 353 NO_3^- from the filters (Malaguti et al., 2015). In this study, the sampling time was from 6:30 am to the next
 354 day 6.30 am. Therefore, the filter-based inorganic measurements suffered from a negative sampling
 355 artifact due to the evaporation of nitrate collected during the forenoon in a temperature of 20°C - 25°C
 356 during the winter campaign and $\sim 38^\circ\text{C}$ - 45°C during the summer campaign.

357 Table 2. Regression coefficients and slopes for the comparison of WSIS measured by HR-ToF-AMS and
 358 IC.

Sites	NO_3^-		SO_4^{2-}		NH_4^+		Cl^-	
	R^2	Slope	R^2	Slope	R^2	Slope	R^2	Slope
IITD Summer	0.42	1.78	0.93	0.17	0.91	0.49	0.55	0.33
IITD Winter	0.82	0.49	0.82	0.68	0.76	0.99	0.82	0.79
IITMD Winter	0.91	1.07	0.93	0.93	0.89	0.93	0.82	0.88

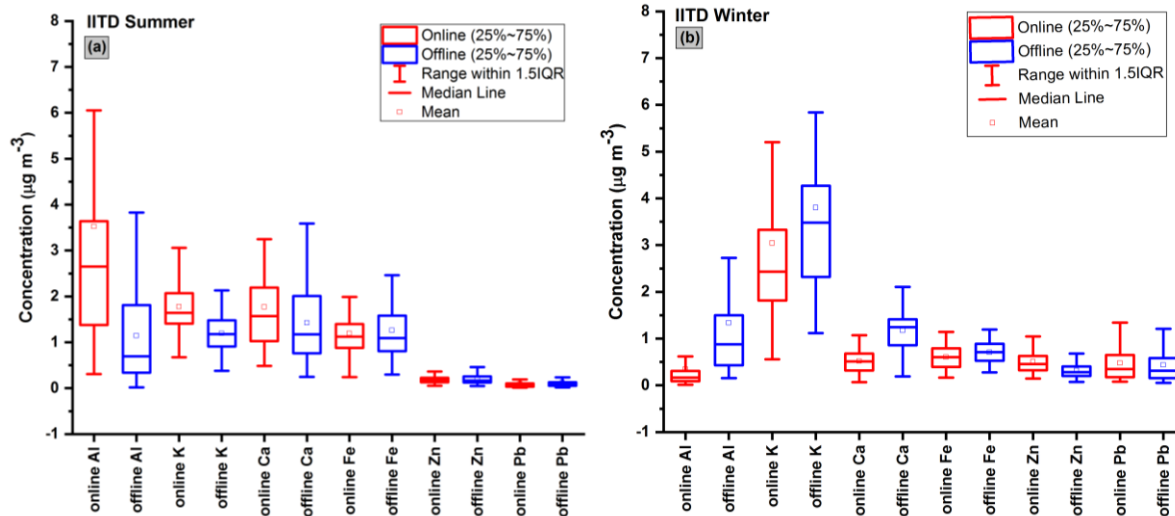
359 We observed higher Cl^- concentration in filter-based measurement than online measurement using HR-
 360 ToF-AMS during both campaigns at IITD and winter at IITMD. A good correlation of $R^2= 0.82$ with a
 361 slope of 0.79 and $R^2= 0.82$ with a slope of 0.88 was observed during the winter campaign at IITD and
 362 IITMD, respectively (Fig. 3). Interestingly, during the summer campaign at IITD the comparability was
 363 moderate with a correlation coefficient of $R^2= 0.55$ and a slope of 0.33. A correlation coefficient of $R^2=$
 364 0.83 between $\text{Dp} < 10 \mu\text{m}$ measured with the MARGA and analyzed from Teflon filters was reported in
 365 Makkonen et al., (2012) during Feb-May. Lower temperature and higher RH during winter retains Cl^- in
 366 particulate phase for long enough to be detected which is not the case in summer. Further, Cl^- is

367 predominantly found in the coarse fraction. Also, while AMS only measures the NR-Cl⁻ (Manchanda et
368 al., 2021), e.g. NH₄Cl, which can vaporize at 600°C but cannot measure Cl⁻ from refractory-KCl, IC
369 measures chloride from all the water-soluble chloride salts, including NH₄Cl and KCl. This probably
370 justifies the lower concentration of Cl⁻ in online measurement from AMS than filter-based measurements.
371 We also compared Cl⁻ measurements from Xact 625i with the measurements from IC. Interestingly, IC
372 measurements of Cl⁻ were found to be higher than Xact 625i measurements during summer at IITD and
373 winter at IITMD. The Cl measurements from Xact 625i were ~1.9 times higher than the measurements
374 from IC during winter at IITD (see fig. SM2 in supplementary material). The correlations were found to
375 be good during winter (R²= 0.83 and 0.76 at IITD and IITMD respectively) and worsen during summer
376 (R²= 0.27 at IITD), similar to what we observed for AMS-Cl⁻ and IC-Cl⁻. It could be due to the
377 differences in water-soluble fraction of chloride in the samples, as ionic concentration (IC) represents
378 water-soluble fraction whereas elemental concentration (Xact 625i) represents total concentration. Also, a
379 lot particulate bound chloride in the atmosphere is in the form of ammonium chloride (Manchanda et al.,
380 2021). Part of the ammonium chloride collected during the day long offline sampling would have
381 vaporized, giving lower concentration from IC measurements. Further investigation is needed to draw a
382 firm conclusion.

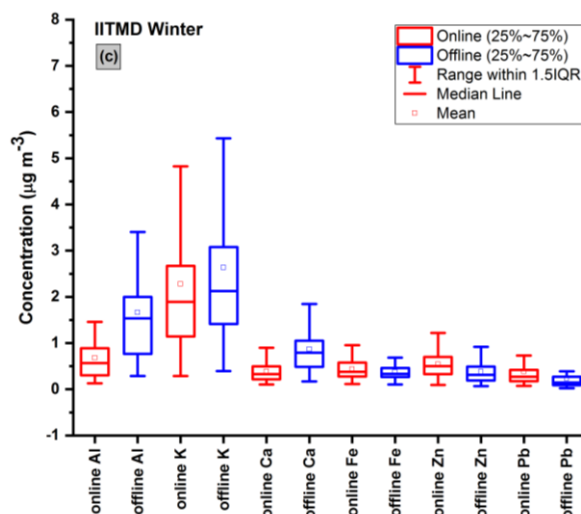
383 **3.2 Online and offline measurements of heavy and trace metals and their comparison**

384 For the inter-comparison of heavy and trace metal concentrations from Xact 625i and ICP-MS, the half-
385 hourly Xact 625i data were averaged to 24 hours filter sampling interval. A total of 32 elements were
386 analyzed on each filter using ICP-MS while, 27 elements were measured in Xact 625i at IITD during
387 summer and winter campaign, and 30 elements were measured in Xact 625i at IITMD during the winter
388 campaign. The spatial and temporal variations of the crustal and trace elements are shown in Fig. SM3. Al
389 and Ca concentrations were the most abundant in ICP-MS and Xact measurements respectively during the
390 summer season (Fig. 4a, 5a & 5b) because of the increase in the crustal activities whereas K
391 concentrations were significantly high for both the measurements during winter (Fig. 4d, 4g, 5c, 5d, 5e
392 and 5f) due to mass-scale agricultural crop-residue burning in the adjoining states of Punjab and Haryana.
393 Elements emitted from anthropogenic activities, e.g., coal-fired power plants (As, Se, Hg, Pb), traffic
394 emissions (Cr, Pb, Mn), wear debris emission (Cu, Cd, Fe, Ga, Mn, Mo), etc. are found to be in higher
395 concentration during winter campaign than summer campaign for both the measurements. Similar results
396 were observed in our companion paper Shukla et al. (2021). The average values of metals along with their
397 ranges are tabulated in Table SM2 and the statistics involved mean, upper, and lower values of some
398 major elements are shown in Fig. 4. Box plots for rest of the metals can be found in Fig. SM4.

399



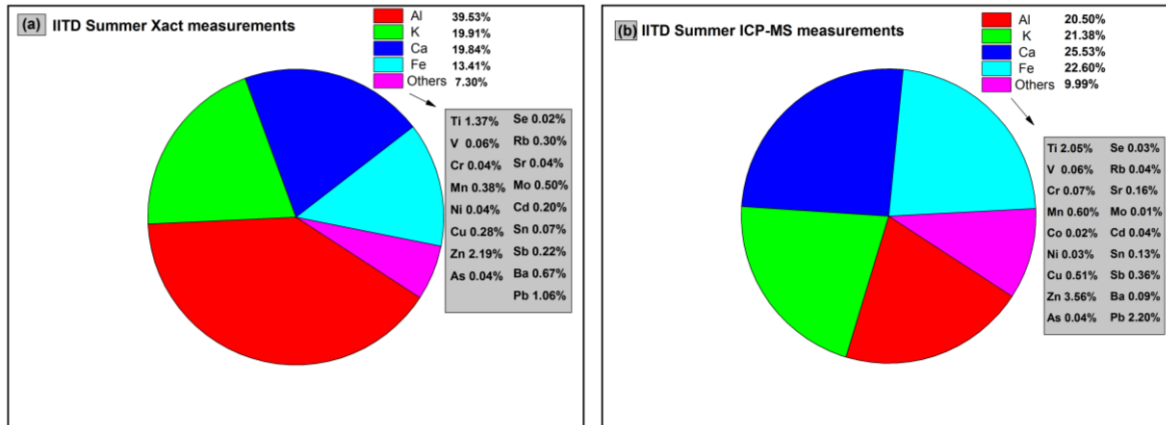
400



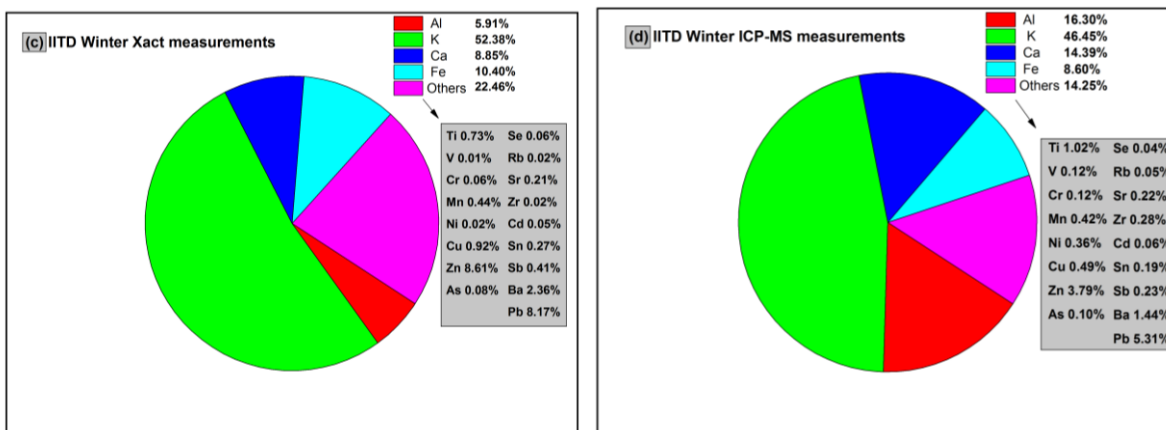
401 Fig.4. Box plots of some major elements measured offline and online during (a) summer campaign at
402 IITD, (b) winter campaign at IITD, and (c) winter campaign at IITMD site. The box plots for rest of the
403 heavy and trace elements are shown in fig. SM4 of the supplementary material.

404 The trends of the elemental concentration in decreasing order for both ICP-MS and Xact measurements
405 during summer and winter at IITD and winter at IITMD are shown in Fig. SM5. The trace metals such as
406 Cd, Mn, Mo, Ba, Pd etc. contribute a small portion in PM_{2.5} in terms of their mass concentration but have
407 a significant effect on human health. Fractions of elements in total element concentration for both the
408 measurements during summer and winter campaign at IITD and during winter campaign at IITMD were
409 shown in Fig. 5.

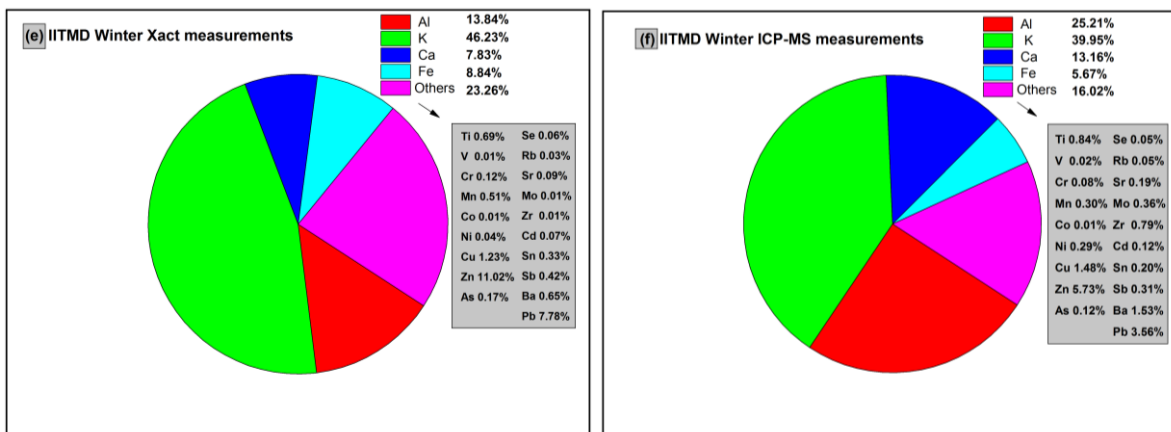
410



411



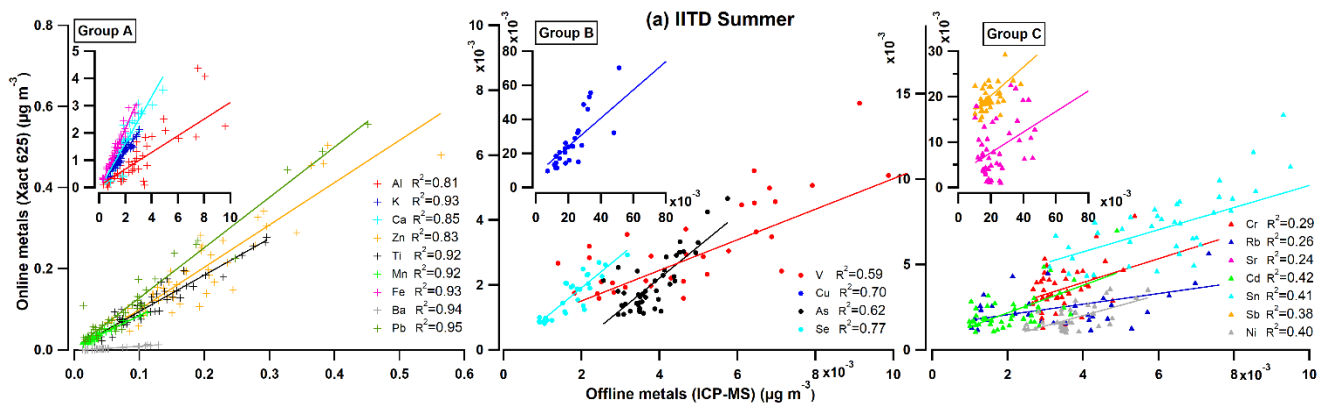
412



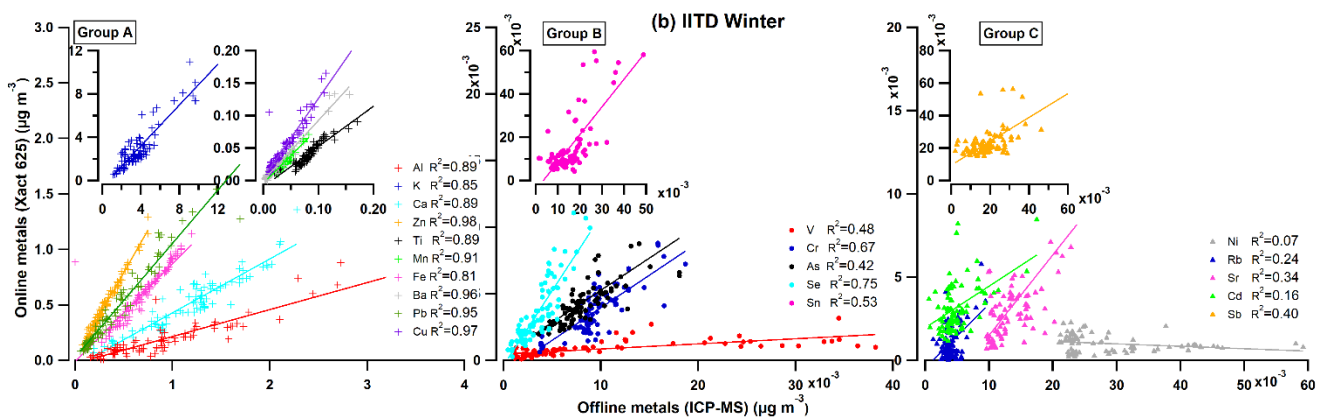
413 Fig.5. Fractions (%) of elements in total element concentration in $PM_{2.5}$ presented in pie format for online
414 (a,c,e) and offline (b,d,f) measurements during winter and summer at IITD and during winter at IITMD.

415 MDLs for ICP-MS measurements were calculated according to Escrig Vidal et al., (2009), and MDLs for
416 Xact 625i were obtained from the manufacturer. MDLs for the Xact 625i and ICP-MS are listed in Table

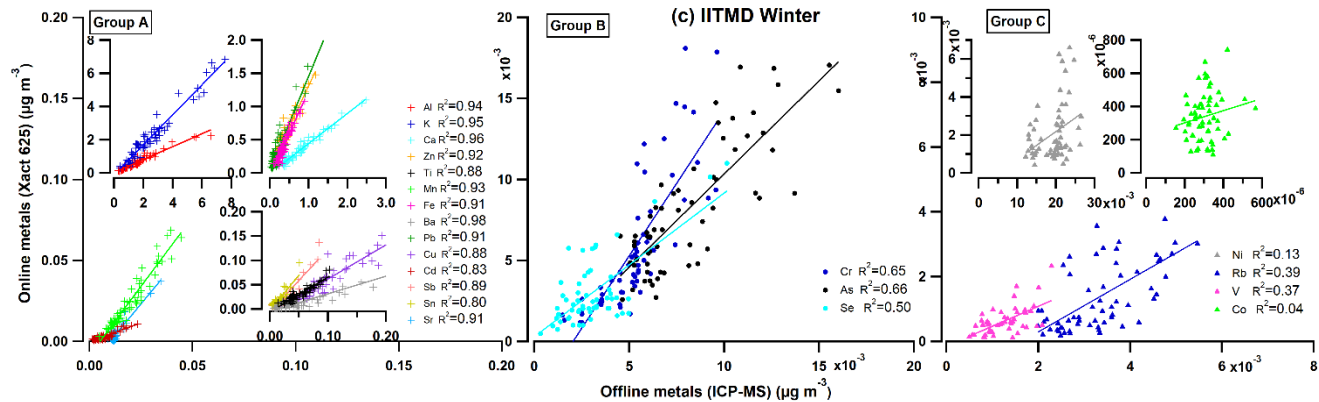
417 SM2 in the supplementary material. Though the half-hourly Xact data were averaged to 24 hours to the
 418 corresponding interval of the filter sampling, for comparability check, MDLs of Xact 625i measurements
 419 were taken for 30 mins sampling time while MDLs of filter-based elemental measurements were
 420 calculated for 24 hours. Elements having data below $3 \times \text{MDL}$ were discarded from further examination
 421 and unreliable as values below $3 \times \text{MDL}$ would lead to higher uncertainty (Furger et al., 2017). The
 422 elements K, Ca, Ti, Mn, Fe, Ba, and Pb have $>80\%$ of their values above both offline and online MDLs,
 423 and thus the data quality is reliable. Further, Ni, Mo, Zr have higher blank concentrations, and thus the
 424 data is not reliable for ICP-MS measurements. The comparability of the elements measured online using
 425 Xact 625i with those analysed using an ICP-MS, was checked for the common elements in these two
 426 measurements (21 elements for IITD and 23 elements for IITMD) and is shown in Fig. 6.



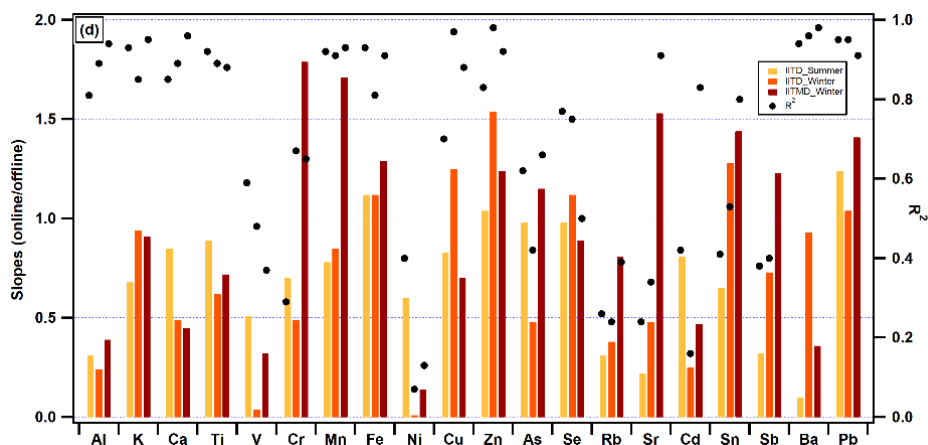
427



428



429



430

431 Fig. 6. Scatter plots and regression lines of Xact 625i vs. ICP-MS data for groups A, B, and C during (a)
 432 summer at IITD, (b) winter at IITD, (c) winter at IITMD, and (d) comparison of slopes (online/offline) &
 433 R^2 of the measured heavy and trace metals in $PM_{2.5}$ during the summer and winter campaign at IITD and
 434 winter campaign at IITMD.

435 Based on their comparability characteristics, elements were grouped under 3 categories. Group A showed
 436 excellent linearity between the two methods with a correlation coefficient of $R^2 > 0.8$. Overall, group A
 437 consists of Al, K, Ca, Ti, Mn, Fe, Cu, Zn, Ba, and Pb during winter at IITD whereas, Cu showed in
 438 another group during summer at IITD. Though Sr, Cd, Sn, Sb had average values below MDLs and posed
 439 a lower correlation coefficient at IITD, interestingly, Sr, Cd, Sn, and Sb joined group A during winter at
 440 IITMD. To distinguish the potential difference in accuracy between the two methods, intercepts were not
 441 forced to be zero. The slopes are important, which indicate biases between the two measurements. The
 442 slopes of Zn, Fe, and Pb were closer to unity during summer at IITD (Fig. 6). K, Fe, Cu, Zn, Ba, and Pb
 443 achieved a slope of 0.94-1.25 during winter at IITD whereas, Mn, Fe, Zn, Pb, Sr, Sn, and Sb pose a slope
 444 slightly higher than unity during winter at IITMD (Fig. 6). A slight difference in cut-off value for the

445 particle size can reduce the slopes from unity and produce ~10% difference in collected mass (Panteliadis
 446 et al., 2012). The slopes and the correlation coefficients are listed in Table 3.

447 In a comparison study conducted by USEPA & Etv. (2012) between Xact 625i and ICP-MS
 448 measurements, Ca, Cu, Mn, Pb, Se, and Zn were highly correlated except Cu. Cu was close to the MDL
 449 values of ICP-MS and Xact 625i. A good agreement was observed between Xact 625i and offline
 450 measurements using ED-XRF in South Korea by Park et al., (2014). The comparability between Xact
 451 measurements and ICP-MS measurements was checked for the elements As, Ba, Ca, Cr, Cu, Fe, K, Mn,
 452 Ni, Pb, Se, Sr, Ti, V, and Zn in Tremper et al. (2018). They observed an average R^2 of 0.93 and a slope of
 453 1.07 for these elements. In the study by Furger et al., (2017) during a warmer season in Switzerland, an
 454 excellent correlation ($R^2 > 0.95$) was found for Xact and ICP-OES/MS measurements of S, K, Ca, Ti, Mn,
 455 Fe, Cu, Zn, Ba, and Pb. However, they found that the elemental measurements by Xact 625i were 28%
 456 higher than ICP-OES/MS measurements for these 10 elements. In our study, Xact measurements of Fe,
 457 Cu, Zn, and Pb yielded an average of 24% higher mass concentrations than ICP-MS measurements for
 458 Group A elements during winter at IITD. Xact measurements were systematically 10% (average) higher
 459 than ICP for Zn, Fe, and Pb during summer at IITD, whereas; we obtained an average of 41% higher
 460 Xact measurements than ICP for Mn, Fe, Zn, Pb, Sr, Sn, and Sb during winter at IITMD in Group A
 461 elements.

462 Group B was characterized by moderate linearity having $R^2 \sim 0.4-0.8$ and consisted of the elements V, Cu,
 463 As, and Se during summer at IITD; V, Cr, As, Se, Sn during winter at IITD and Cr, As and Se during
 464 winter at IITMD. These elements in Group B had their values very close to or below MDLs of at least
 465 one of the analysis methods. During winter at both sites, Cr and As from ICP-MS have ~50-65% of their
 466 values below MDLs, whereas ~68-72% of their values were above the MDLs of Xact 625i. Though some
 467 of the elements in this group in different seasons have slopes near or greater than unity (see Table 3) like
 468 Group A, their comparison is not statistically feasible.

469 Table 3. Regression coefficients and slopes for the comparison of Xact 625i and ICP-MS measurements.

Sites	Group A	Slope	R^2	Group B	Slope	R^2	Group C	Slope	R^2
IITD Summer	Al	0.31	0.81	V	0.51	0.59	Cr	0.7	0.29
	K	0.68	0.93	Cu	0.83	0.70	Co	-	-
	Ca	0.85	0.85	As	0.98	0.62	Rb	0.31	0.26
	Zn	1.04	0.83	Se	0.98	0.77	Sr	0.22	0.24
	Ba	0.1	0.94				Mo	-	-

	Ti	0.89	0.92				Cd	0.81	0.42
	Mn	0.78	0.92				Sn	0.65	0.41
	Fe	1.12	0.93				Sb	0.32	0.38
	Pb	1.24	0.95				Ni	0.6	0.4
IITD Winter	Al	0.24	0.89	V	0.04	0.48	Ni	0.01	0.07
	K	0.94	0.85	Cr	0.49	0.67	Rb	0.38	0.24
	Ca	0.49	0.89	As	0.48	0.42	Sr	0.48	0.34
	Ti	0.62	0.89	Se	1.12	0.75	Zr	-	-
	Mn	0.85	0.91	Sn	1.28	0.53	Cd	0.25	0.16
	Fe	1.12	0.81				Sb	0.73	0.40
	Cu	1.25	0.97						
	Zn	1.54	0.98						
	Ba	0.93	0.96						
	Pb	1.04	0.95						
IITMD Winter	Al	0.39	0.94	Cr	1.79	0.65	Ni	0.14	0.13
	K	0.91	0.95	As	1.15	0.66	Rb	0.81	0.39
	Ca	0.45	0.96	Se	0.89	0.5	Mo	-	-
	Ti	0.72	0.88				Zr	-	-
	Mn	1.71	0.93				V	0.32	0.37
	Fe	1.29	0.91				Co	0.36	0.04
	Cu	0.70	0.88						
	Zn	1.24	0.92						
	Ba	0.36	0.98						
	Pb	1.41	0.91						
	Sr	1.53	0.91						
	Cd	0.47	0.83						
	Sn	1.44	0.8						
Sb	1.23	0.89							

470 The Group C elements, e.g., Ni, Rb, Sr, Zr, Cd, and Sb during summer at IITD; Cr, Co, Rb, Sr, Mo, Cd,
471 Sn, Sb, and Ni during winter at IITD and, Ni, Rb, Mo, Zr, V, and Co during winter at IITMD are
472 characterized by their bad correlation ($R^2 < 0.4$). Interestingly, measurements of some element e.g. Mo
473 during summer and winter at IITD and IITMD respectively, Co during summer at IITD, and Zr during

474 winter at both sites from both the methods did not correlate at all. For most of the elements in this group,
475 70-85% of measurements were below both method's MDLs and rest of the data were below $3 \times$ MDLs.
476 The high and variable blank concentrations of these elements increased the MDL values in ICP-MS
477 measurement. The particle size dependent self-absorption effect and line interference between different
478 elements in Xact measurement could also increase the MDL values (Furger et al., 2017). This is probably
479 the reason for the values lower than MDLs for the elements in this group.

480 Overall, we observed 10-40% higher Xact measurements than ICP for some of the elements in Group A
481 during different seasons. The difference in the Xact and High-volume sampler inlet location and their
482 distance from the road can cause such difference in measurements (Furger et al., 2017). In the case of dust
483 resuspension from vehicular traffic, the number concentration of finer particulate matter tends to decrease
484 sharply within an increment of just 50m from the roadway (Hagler et al., 2009). In this study, we tried to
485 co-locate the two sample inlets, but it could not be avoided. Also, IITD and IITMD are both very close
486 (<200 m) to a roadway with moderate to heavy-duty traffic. The differences in online and offline
487 measurements may indicate a gradient in some elements due to very close proximity to heavy-duty traffic.
488 Also, the different temperatures of the sample inlets may give rise to a difference in measured
489 concentrations from both methods (Tremper et al., 2018). In this study, the blank corrected ICP-MS
490 measurements may result in overestimation or underestimation due to variable and high blank
491 concentration. The difference can also occur due to the digestion recovery rate for the digestion protocol
492 used for the filter analysis. Moreover, if the ambient elemental concentration is much lower than the
493 standards used for calibration of Xact, such differences may occur (Indresand et al., 2013).

494 **4. Conclusion**

495 Atmospheric WSIS (NO_3^- , SO_4^{2-} , NH_4^+ , Cl^-) and heavy and trace elements in $\text{PM}_{2.5}$ were measured using
496 offline methods (IC for WSIS and ICP-MS for elements) and online methods (HR-ToF-AMS for
497 inorganics and Xact 625i for elements). These measurements were compared to assess the measurement
498 quality and sampling artifacts of these measurement techniques in the heavily polluted Delhi-NCR for
499 two different metrological conditions (winter and summer season). Field campaigns were conducted at
500 two NCR sites, namely, IITD during June-July 2019 and Oct-Dec 2019 and at IITMD during Oct-Dec
501 2019. The key findings of this study are summarized below.

- 502 • NH_4^+ concentrations from the IC and HR-ToF-AMS, compared well during winter with a slope
503 of 0.99 at IITD and 0.93 at IITMD. Interestingly, NH_4^+ concentrations were higher in offline

504 measurements during summer at IITD. The decrease in slope was probably due to the formation
505 of particulate $(\text{NH}_4)_2\text{SO}_4$.

- 506 • Offline SO_4^{2-} measurements were higher (with a slope of 0.17 during summer at IITD and 0.8
507 and 0.93 during winter at IITD and IITMD, respectively) during both seasons at both the sites
508 due to the positive sampling artifact. The absorption of SO_2 and the oxidation or condensation
509 process may result in additional sulphate.
- 510 • Lower NO_3^- concentrations (with a slope of 1.78 during summer at IITD and 1.07 during winter
511 at IITMD) were observed in the offline measurement during summer at IITD and during winter
512 at IITMD because of the evaporation of NH_4NO_3 from the filter substrates. The evaporative
513 loss of nitrate from the filters was minimal in winter at IITMD. It aggravated during summer at
514 IITD due to the evaporation of ammonium nitrate in such a high temperature (35°C - 48°C) range.
515 The higher NO_3^- concentrations (slope~0.49) in the filters than HR-ToF-AMS measurements
516 during winter at IITD can be due to the absorption of gas-phase HNO_3 on the filter.
- 517 • Offline Cl^- was consistently higher (with a slope of 0.33 during summer at IITD and 0.79 and
518 0.88 during winter at IITD and IITMD, respectively) than HR-ToF-AMS measurements during
519 both seasons at both sites mainly because HR-ToF-AMS only measures the NR- Cl^- whereas, the
520 offline Cl^- measurements includes chloride from all the water-soluble chloride salts. The
521 comparability degrades during summer due to the volatile nature of Cl^- in higher temperatures
522 and lower RH.
- 523 • The elements were grouped into three categories (Group A, B and C) according to their
524 comparability characteristics. The elemental data from Xact 625i were highly correlated
525 ($R^2>0.8$) with ICP-MS measurements of the 24 hr filters for Group A elements (Al, K, Ca, Ti,
526 Zn, Mn, Fe, Ba, and Pb). The Cu also showed up in this group during winter at IITD. About
527 80% of the data for these elements were above MDLs for both the methods. Though Sn, Sb, and
528 Cd had values below MDLs of one or both the methods, interestingly, they were highly
529 correlated ($R^2>0.8$) and, slopes are very close to unity for Sn and Sb during winter at IITMD.
530 The correlation coefficients > 0.8 for the elements in Group A indicated the high precision of
531 the online and offline measurements. Hence, these elements from any of these methods can be
532 reliably used for modelling studies.
- 533 • The elements under Group B had their values closer to or below at least one of the method's
534 MDLs. Cr and As had ~50-65% of their values below ICP-MS MDLs from ICP-MS, whereas
535 ~68-72% of their values were above Xact 625i MDLs during winter at both sites.

- 536 • Elements like Ni, Mo, and Zr measured from ICP-MS were not reliable due to their higher and
537 variable blank concentrations. No conclusion on their measurement accuracy by the two
538 methods can be drawn.
- 539 • In summary, the daily averaged half-hourly Xact 625i measurements were 10-40% higher than
540 24 hr filter measurements by ICP-MS depending upon the seasons, sites and elements in Group
541 A. Distance between two inlets for the two methods, distance of the inlets from the roadway,
542 line interference between two elements in Xact measurements, particle size, sampling strategy,
543 filter type, higher and variable concentrations in blank filters and digestion protocol for ICP
544 measurements can cause the difference in measurements between the two methods.

545 The above findings highlight the measurement methods' accuracy and implement the particular type of
546 measurements as needed. Denuders could be effective in avoiding the overestimation problems of
547 ammonium and sulphate in filter measurements and improve the comparison. Also, teflon filters instead
548 of quartz filters in the un-denuded sampler are reported to give better comparison for sulphate. The MDLs
549 in the Xact 625 measurements are higher than the MDLs for the offline method. Depending on the
550 objective of the campaign, Xact 625 can be deployed for a longer time interval to analyse the elements
551 that are below their MDLs. The high resolution real-time monitoring of non-refractory organics,
552 inorganics by HR-ToF-AMS and elements by Xact comes at the cost of high sensitivity in MDLs,
553 calibrations and cost. Whereas, cost effectiveness of conventional samplers makes it practical to deploy in
554 larger numbers at multi-sites simultaneously. Overall, high resolution real time sampling provides a rich
555 dataset for high and small pollution episodes. Future work should involve using different filter substrates
556 and different digestion protocols to re-evaluate the difference between these online and offline methods.
557 Although this study compares the PM species, a comparison of full source apportionment analysis
558 between online and offline methods should be done for more qualitative and quantitative insights.

559 **Author contribution**

560 HSB performed the offline analysis, data processing and wrote the manuscript. JD collected the AMS
561 data at IITD. AS and VL carried out the Xact and AMS data collection and processing respectively. NR,
562 MK, VS and SNT were involved with the supervision and conceptualization. All co-authors contributed
563 to the paper discussion and revision.

564 **Declaration of interests**

565 The authors declare that they have no conflict of interest.

566 **Acknowledgements**

567 The authors are thankful to Naba Hazarika and Mohd Faisal for collecting the Xact data at IITMD and
568 Pawan Vats for the sampling and collection of the filters at IITD. The authors are also thankful to Amit
569 Vishwakarma, Vaibhav Shrivastava and Harishankar for helping in offline analysis. This work is
570 financially supported by the Department of Biotechnology, Government of India (Grant No.
571 BT/IN/UK/APHH/41/KB/2016-17 dated 19th July 2017) and Central Pollution Control Board (CPCB),
572 Government of India to conduct this research under grant no. AQM/Source apportionment_EPC
573 Project/2017 dated 12th February 2019.

574 **Reference**

575 Bhowmik, H. S., Naresh, S., Bhattu, D., Rastogi, N., Prévôt, A. S. H. and Tripathi, S. N.: Temporal and spatial
576 variability of carbonaceous species (EC; OC; WSOC and SOA) in PM_{2.5} aerosol over five sites of Indo-Gangetic
577 Plain, *Atmos. Pollut. Res.*, 12(June 2020), 375–390, doi:10.1016/j.apr.2020.09.019, 2020.

578 Chow, J. C.: Measurement methods to determine compliance with ambient air quality standards for suspended
579 particles, *J. Air Waste Manag. Assoc.*, 45(5), 320–382, doi:10.1080/10473289.1995.10467369, 1995.

580 Chow, J. C., Watson, J. G., Lowenthal, D. H., Park, K., Doraiswamy, P., Bowers, K. and Bode, R.: Continuous and
581 filter-based measurements of PM_{2.5} nitrate and sulfate at the Fresno Supersite, *Environ. Monit. Assess.*, 144(1–3),
582 179–189, doi:10.1007/s10661-007-9987-5, 2008.

583 DeCarlo, P. F., Kimmel, J. R., Trimborn, A., Northway, M. J., Jayne, J. T., Aiken, A. C., Gonin, M., Fuhrer, K.,
584 Horvath, T., Docherty, K. S., Worsnop, D. R. and Jimenez, J. L.: Field-deployable, high-resolution, time-of-flight
585 aerosol mass spectrometer, *Anal. Chem.*, 78(24), 8281–8289, doi:10.1021/ac061249n, 2006.

586 Escrig Vidal, A., Monfort, E., Celades, I., Querol, X., Amato, F., Minguillón, M. C. and Hopke, P. K.: Application
587 of optimally scaled target factor analysis for assessing source contribution of ambient PM₁₀, *J. Air Waste Manag.*
588 *Assoc.*, 59(11), 1296–1307, doi:10.3155/1047-3289.59.11.1296, 2009.

589 Furger, M., Minguillón, M. C., Yadav, V., Slowik, J. G., Hüglin, C., Fröhlich, R., Petterson, K., Baltensperger, U.
590 and Prévôt, A. S. H.: Elemental composition of ambient aerosols measured with high temporal resolution using an
591 online XRF spectrometer, *Atmos. Meas. Tech.*, 10(6), 2061–2076, doi:10.5194/amt-10-2061-2017, 2017.

592 Gani, S., Bhandari, S., Seraj, S., Wang, D. S., Patel, K., Soni, P., Arub, Z., Habib, G., Hildebrandt Ruiz, L. and
593 Apte, J. S.: Submicron aerosol composition in the world's most polluted megacity: The Delhi Aerosol Supersite
594 study, *Atmos. Chem. Phys.*, 19(10), 6843–6859, doi:10.5194/acp-19-6843-2019, 2019.

595 Hagler, G. S. W., Baldauf, R. W., Thoma, E. D., Long, T. R., Snow, R. F., Kinsey, J. S., Oudejans, L. and Gullett,

596 B. K.: Ultrafine particles near a major roadway in Raleigh, North Carolina: Downwind attenuation and correlation
597 with traffic-related pollutants, *Atmos. Environ.*, 43(6), 1229–1234, doi:10.1016/j.atmosenv.2008.11.024, 2009.

598 Hong, C., Zhang, Q., Zhang, Y., Davis, S. J., Tong, D., Zheng, Y., Liu, Z., Guan, D., He, K. and Schellnhuber, H. J.:
599 Impacts of climate change on future air quality and human health in China, *Proc. Natl. Acad. Sci. U. S. A.*, 116(35),
600 17193–17200, doi:10.1073/pnas.1812881116, 2019.

601 Hu, W., Campuzano-Jost, P., Day, D. A., Croteau, P., Canagaratna, M. R., Jayne, J. T., Worsnop, D. R. and
602 Jimenez, J. L.: Evaluation of the new capture vaporizer for aerosol mass spectrometers (AMS) through field studies
603 of inorganic species, *Aerosol Sci. Technol.*, 51(6), 735–754, doi:10.1080/02786826.2017.1296104, 2017.

604 Indresand, H., White, W. H., Trzepla, K. and Dillner, A. M.: Preparation of sulfur reference materials that reproduce
605 atmospheric particulate matter sample characteristics for XRF calibration, *X-Ray Spectrom.*, 42(5), 359–367,
606 doi:10.1002/xrs.2456, 2013.

607 Jayne, J. T., Leard, D. C., Zhang, X., Davidovits, P., Smith, K. A., Kolb, C. E. and Worsnop, D. R.: Development of
608 an aerosol mass spectrometer for size and composition analysis of submicron particles, *Aerosol Sci. Technol.*, 33(1–
609 2), 49–70, doi:10.1080/027868200410840, 2000.

610 Jimenez, J. L., Jayne, J. T., Shi, Q., Kolb, C. E., Worsnop, D. R., Yourshaw, I., Seinfeld, J. H., Flagan, R. C., Zhang,
611 X., Smith, K. A., Morris, J. W. and Davidovits, P.: Ambient aerosol sampling using the Aerodyne aerosol mass
612 spectrometer, *J. Geophys. Res. Atmos.*, 108(7), doi:10.1029/2001jd001213, 2003.

613 Lalchandani, V., Kumar, V., Tobler, A., M. Thamban, N., Mishra, S., Slowik, J. G., Bhattu, D., Rai, P., Satish, R.,
614 Ganguly, D., Tiwari, S., Rastogi, N., Tiwari, S., Močnik, G., Prévôt, A. S. H. and Tripathi, S. N.: Real-time
615 characterization and source apportionment of fine particulate matter in the Delhi megacity area during late winter,
616 *Sci. Total Environ.*, 770, doi:10.1016/j.scitotenv.2021.145324, 2021.

617 Lalchandani, V., Srivastava, D., Dave, J., Mishra, S., Tripathi, N., Shukla, A. K., Sahu, R., Thamban, N. M.,
618 Gaddamidi, S., Dixit, K., Ganguly, D., Tiwari, S., Srivastava, A. K., Sahu, L., Rastogi, N., Gargava, P. and Tripathi,
619 S. N.: Effect of Biomass Burning on PM_{2.5} Composition and Secondary Aerosol Formation During Post-Monsoon
620 and Winter Haze Episodes in Delhi, *J. Geophys. Res. Atmos.*, 127(1), 1–21, doi:10.1029/2021JD035232, 2022.

621 Lipfert, F. W.: Filter artifacts associated with particulate measurements: Recent evidence and effects on statistical
622 relationships, *Atmos. Environ.*, 28(20), 3233–3249, doi:10.1016/1352-2310(94)00167-J, 1994.

623 Makkonen, U., Virkkula, A., Mäntykenttä, J., Hakola, H., Keronen, P., Vakkari, V. and Aalto, P. P.: Semi-
624 continuous gas and inorganic aerosol measurements at a Finnish urban site: Comparisons with filters, nitrogen in
625 aerosol and gas phases, and aerosol acidity, *Atmos. Chem. Phys.*, 12(12), 5617–5631, doi:10.5194/acp-12-5617-
626 2012, 2012.

627 Malaguti, A., Mircea, M., La Torretta, T. M. G., Telloli, C., Petralia, E., Stracquadanio, M. and Berico, M.:

628 Comparison of online and offline methods for measuring fine secondary inorganic ions and carbonaceous aerosols in
629 the central mediterranean area, *Aerosol Air Qual. Res.*, 15(7), 2641–2653, doi:10.4209/aaqr.2015.04.0240, 2015.

630 Manchanda, C., Kumar, M., Singh, V., Faisal, M., Hazarika, N., Shukla, A., Lalchandani, V., Goel, V., Thamban,
631 N., Ganguly, D. and Tripathi, S. N.: Variation in chemical composition and sources of PM_{2.5} during the COVID-19
632 lockdown in Delhi, *Environ. Int.*, 153(December 2020), 106541, doi:10.1016/j.envint.2021.106541, 2021.

633 Minguillón, M. C., Querol, X., Baltensperger, U. and Prévôt, A. S. H.: Fine and coarse PM composition and sources
634 in rural and urban sites in Switzerland: Local or regional pollution?, *Sci. Total Environ.*, 427–428, 191–202,
635 doi:10.1016/j.scitotenv.2012.04.030, 2012.

636 Nagar, P. K., Singh, D., Sharma, M., Kumar, A., Aneja, V. P., George, M. P., Agarwal, N. and Shukla, S. P.:
637 Characterization of PM_{2.5} in Delhi: role and impact of secondary aerosol, burning of biomass, and municipal solid
638 waste and crustal matter, *Environ. Sci. Pollut. Res.*, 24(32), 25179–25189, doi:10.1007/s11356-017-0171-3, 2017.

639 Nault, B. A., Campuzano-Jost, P., Day, D. A., Guo, H., Jo, D. S., Handschy, A. V., Pagonis, D., Schroder, J. C.,
640 Schueneman, M. K., Cubison, M. J., Dibb, J. E., Hodzic, A., Hu, W., Palm, B. B. and Jimenez, J. L.: Interferences
641 with aerosol acidity quantification due to gas-phase ammonia uptake onto acidic sulfate filter samples, *Atmos.*
642 *Meas. Tech.*, 13(11), 6193–6213, doi:10.5194/amt-13-6193-2020, 2020.

643 Nicolás, J. F., Galindo, N., Yubero, E., Pastor, C., Esclapez, R. and Crespo, J.: Aerosol inorganic ions in a semiarid
644 region on the Southeastern Spanish mediterranean coast, *Water. Air. Soil Pollut.*, 201(1–4), 149–159,
645 doi:10.1007/s11270-008-9934-2, 2009.

646 Nie, W., Wang, T., Gao, X., Pathak, R. K., Wang, X., Gao, R., Zhang, Q., Yang, L. and Wang, W.: Comparison
647 among filter-based, impactor-based and continuous techniques for measuring atmospheric fine sulfate and nitrate,
648 *Atmos. Environ.*, 44(35), 4396–4403, doi:10.1016/j.atmosenv.2010.07.047, 2010.

649 Pakkanen, T. A. and Hillamo, R. E.: Comparison of sampling artifacts and ion balances for a Berner low-pressure
650 impactor and a virtual impactor, *Boreal Environ. Res.*, 7(2), 129–140, 2002.

651 Pandolfi, M., Querol, X., Alastuey, A., Jimenez, J. L., Jorba, O., Day, D., Ortega, A., Cubison, M. J., Comerón, A.,
652 Sicard, M., Mohr, C., Prévôt, A. S. H., Minguillón, M. C., Pey, J., Baldasano, J. M., Burkhardt, J. F., Seco, R.,
653 Peñuelas, J., Van Drooge, B. L., Artiñano, B., DiMarco, C., Nemitz, E., Schallhart, S., Metzger, A., Hansel, A.,
654 Lorente, J., Ng, S., Jayne, J. and Szidat, S.: Effects of sources and meteorology on particulate matter in the Western
655 Mediterranean Basin: An overview of the DAURE campaign, *J. Geophys. Res.*, 119(8), 4978–5010,
656 doi:10.1002/2013JD021079, 2014.

657 Pant, P., Shukla, A., Kohl, S. D., Chow, J. C., Watson, J. G. and Harrison, R. M.: Characterization of ambient
658 PM_{2.5} at a pollution hotspot in New Delhi, India and inference of sources, *Atmos. Environ.*, 109, 178–189,
659 doi:10.1016/j.atmosenv.2015.02.074, 2015.

660 Panteliadis, P., Helmink, H. J. P., Koopman, P. C., Hoonhout, M., Jonge, D. De and Visser, J. H.: PM 10 sampling
661 inlets comparison : EPA vs EU , 12341(1999), 12341, 2012.

662 Park, S. S., Cho, S. Y., Jo, M. R., Gong, B. J., Park, J. S. and Lee, S. J.: Field evaluation of a near-real time
663 elemental monitor and identification of element sources observed at an air monitoring supersite in Korea, *Atmos.*
664 *Pollut. Res.*, 5(1), 119–128, doi:10.5094/APR.2014.015, 2014.

665 Patel, A., Rastogi, N., Gandhi, U. and Khatri, N.: Oxidative potential of atmospheric PM10 at five different sites of
666 Ahmedabad, a big city in Western India, *Environ. Pollut.*, 268, 115909, doi:10.1016/j.envpol.2020.115909, 2021.

667 Pathak, R. K. and Chan, C. K.: Inter-particle and gas-particle interactions in sampling artifacts of PM2.5 in filter-
668 based samplers, *Atmos. Environ.*, 39(9), 1597–1607, doi:10.1016/j.atmosenv.2004.10.018, 2005.

669 Peck, J., Gonzalez, L. A., Williams, L. R., Xu, W., Croteau, P. L., Timko, M. T., Jayne, J. T., Worsnop, D. R.,
670 Miake-Lye, R. C. and Smith, K. A.: Development of an aerosol mass spectrometer lens system for PM2.5, *Aerosol*
671 *Sci. Technol.*, 50(8), 781–789, doi:10.1080/02786826.2016.1190444, 2016.

672 Pope, C. A., Ezzati, M. and Dockery, D. W.: Fine-Particulate Air Pollution and Life Expectancy in the United
673 States, *N. Engl. J. Med.*, 360(4), 376–386, doi:10.1056/nejmsa0805646, 2009.

674 Querol, X., Pey, J., Minguillón, M. C., Pérez, N., Alastuey, A., Viana, M., Moreno, T., Bernabé, R. M., Blanco, S.,
675 Cárdenas, B., Vega, E., Sosa, G., Escalona, S., Ruiz, H. and Artíñano, B.: PM speciation and sources in Mexico
676 during the MILAGRO-2006 campaign, *Atmos. Chem. Phys.*, 8(1), 111–128, doi:10.5194/acp-8-111-2008, 2008.

677 Rai, P., Furger, M., El Haddad, I., Kumar, V., Wang, L., Singh, A., Dixit, K., Bhattu, D., Petit, J. E., Ganguly, D.,
678 Rastogi, N., Baltensperger, U., Tripathi, S. N., Slowik, J. G. and Prévôt, A. S. H.: Real-time measurement and
679 source apportionment of elements in Delhi’s atmosphere, *Sci. Total Environ.*, 742,
680 doi:10.1016/j.scitotenv.2020.140332, 2020.

681 Rai, P., Slowik, J. G., Furger, M., El Haddad, I., Visser, S., Tong, Y., Singh, A., Wehrle, G., Kumar, V., Tobler, A.
682 K., Bhattu, D., Wang, L., Ganguly, D., Rastogi, N., Huang, R. J., Necki, J., Cao, J., Tripathi, S. N., Baltensperger,
683 U. and Prevot, A. S. H.: Highly time-resolved measurements of element concentrations in PM10 and PM2.5:
684 Comparison of Delhi, Beijing, London, and Krakow, *Atmos. Chem. Phys.*, 21(2), 717–730, doi:10.5194/acp-21-
685 717-2021, 2021.

686 Rastogi, N. and Sarin, M. M.: Long-term characterization of ionic species in aerosols from urban and high-altitude
687 sites in western India: Role of mineral dust and anthropogenic sources, *Atmos. Environ.*, 39(30), 5541–5554,
688 doi:10.1016/j.atmosenv.2005.06.011, 2005.

689 Rengarajan, R., Sarin, M. M. and Sudheer, A. K.: Carbonaceous and inorganic species in atmospheric aerosols
690 during wintertime over urban and high-altitude sites in North India, *J. Geophys. Res. Atmos.*, 112(21), 1–16,
691 doi:10.1029/2006JD008150, 2007.

692 Schaap, M., Spindler, G., Schulz, M., Acker, K., Maenhaut, W., Berner, A., Wieprecht, W., Streit, N., Müller, K.,
693 Brüggemann, E., Chi, X., Putaud, J. P., Hitzengerger, R., Puxbaum, H., Baltensperger, U. and Ten Brink, H.:
694 Artefacts in the sampling of nitrate studied in the “iINTERCOMP” campaigns of EUROTRAC-AEROSOL, *Atmos.*
695 *Environ.*, 38(38), 6487–6496, doi:10.1016/j.atmosenv.2004.08.026, 2004.

696 Sharma, D. and Kulshrestha, U. C.: Spatial and temporal patterns of air pollutants in rural and urban areas of India,
697 *Environ. Pollut.*, 195(2), 276–281, doi:10.1016/j.envpol.2014.08.026, 2014.

698 Sharma, S. K., Mandal, T. K., Jain, S., Saraswati, Sharma, A. and Saxena, M.: Source Apportionment of PM_{2.5} in
699 Delhi, India Using PMF Model, *Bull. Environ. Contam. Toxicol.*, 97(2), 286–293, doi:10.1007/s00128-016-1836-1,
700 2016.

701 Shukla, A. K., Lalchandani, V., Bhattu, D., Dave, J. S., Rai, P., Thamban, N. M., Mishra, S., Gaddamidi, S.,
702 Tripathi, N., Vats, P., Rastogi, N., Sahu, L., Ganguly, D., Kumar, M., Singh, V., Gargava, P. and Tripathi, S. N.:
703 Real-time quantification and source apportionment of fine particulate matter including organics and elements in
704 Delhi during summertime, *Atmos. Environ.*, 261(July), 118598, doi:10.1016/j.atmosenv.2021.118598, 2021.

705 Singh, A., Satish, R. V. and Rastogi, N.: Characteristics and sources of fine organic aerosol over a big semi-arid
706 urban city of western India using HR-ToF-AMS, *Atmos. Environ.*, 208(April), 103–112,
707 doi:10.1016/j.atmosenv.2019.04.009, 2019.

708 Singh, A., Rastogi, N., Kumar, V., Slowik, J. G., Satish, R., Lalchandani, V., Thamban, N. M., Rai, P., Bhattu, D.,
709 Vats, P., Ganguly, D., Tripathi, S. N. and Prévôt, A. S. H.: Sources and characteristics of light-absorbing fine
710 particulates over Delhi through the synergy of real-time optical and chemical measurements, *Atmos. Environ.*,
711 252(March), doi:10.1016/j.atmosenv.2021.118338, 2021.

712 Singhai, A., Habib, G., Raman, R. S. and Gupta, T.: Chemical characterization of PM_{1.0} aerosol in Delhi and source
713 apportionment using positive matrix factorization, *Environ. Sci. Pollut. Res.*, 24(1), 445–462, doi:10.1007/s11356-
714 016-7708-8, 2017.

715 Takahama, S., Wittig, A. E., Vayenas, D. V., Davidson, C. I. and Pandis, S. N.: Modeling the diurnal variation of
716 nitrate during the Pittsburgh Air Quality Study, *J. Geophys. Res. D Atmos.*, 109(16), doi:10.1029/2003JD004149,
717 2004.

718 Tobler, A., Bhattu, D., Canonaco, F., Lalchandani, V., Shukla, A., Thamban, N. M., Mishra, S., Srivastava, A. K.,
719 Bisht, D. S., Tiwari, S., Singh, S., Močnik, G., Baltensperger, U., Tripathi, S. N., Slowik, J. G. and Prévôt, A. S. H.:
720 Chemical characterization of PM_{2.5} and source apportionment of organic aerosol in New Delhi, India, *Sci. Total*
721 *Environ.*, 745, doi:10.1016/j.scitotenv.2020.140924, 2020.

722 Tremper, A. H., Font, A., Priestman, M., Hamad, S. H., Chung, T. C., Pribadi, A., Brown, R. J. C., Goddard, S. L.,
723 Grassineau, N., Petterson, K., Kelly, F. J. and Green, D. C.: Field and laboratory evaluation of a high time resolution

724 x-ray fluorescence instrument for determining the elemental composition of ambient aerosols, *Atmos. Meas. Tech.*,
725 11(6), 3541–3557, doi:10.5194/amt-11-3541-2018, 2018.

726 Usepa and Etv: Environmental Technology Verification Report Cooper Environmental Services LLC † Xact 625
727 Particulate Metals Monitor, , (September 2012) [online] Available from: <http://cooperenvironmental.com/>, 2012.

728 Viana, M., Chi, X., Maenhaut, W., Cafmeyer, J., Querol, X., Alastuey, A., Mikuška, P. and Večeřa, Z.: Influence of
729 sampling artefacts on measured PM, OC, and EC levels in carbonaceous aerosols in an urban area, *Aerosol Sci.*
730 *Technol.*, 40(2), 107–117, doi:10.1080/02786820500484388, 2006.

731 Wang, M., Aaron, C. P., Madrigano, J., Hoffman, E. A., Angelini, E., Yang, J., Laine, A., Vetterli, T. M., Kinney, P.
732 L., Sampson, P. D., Sheppard, L. E., Szpiro, A. A., Adar, S. D., Kirwa, K., Smith, B., Lederer, D. J., Diez-Roux, A.
733 V., Vedal, S., Kaufman, J. D. and Barr, R. G.: Association between long-term exposure to ambient air pollution and
734 change in quantitatively assessed emphysema and lung function, *JAMA - J. Am. Med. Assoc.*, 322(6), 546–556,
735 doi:10.1001/jama.2019.10255, 2019.

736 Wu, W. S. and Wang, T.: On the performance of a semi-continuous PM_{2.5} sulphate and nitrate instrument under
737 high loadings of particulate and sulphur dioxide, *Atmos. Environ.*, 41(26), 5442–5451,
738 doi:10.1016/j.atmosenv.2007.02.025, 2007.

739 Zhang, D., Shi, G. Y., Iwasaka, Y. and Hu, M.: Mixture of sulfate and nitrate in coastal atmospheric aerosols:
740 Individual particle studies in Qingdao (36°04'N, 120°21'E), China, *Atmos. Environ.*, 34(17), 2669–2679,
741 doi:10.1016/S1352-2310(00)00078-9, 2000.

742 Zhang, X. and McMurry, P. H.: EVAPORATIVE LOSSES OF FINE PARTICULATE NITRATES DURING
743 SAMPLING., 1992.

744